www.czasopisma.pan.pl PAN POLSKA AKADEMIA NAUK www.journals.pan.pl

Arch. Min. Sci. **68** (2023), 1, 71-86

Electronic version (in color) of this paper is available: http://mining.archives.pl

DOI: https://doi.org/10.24425/ams.2023.144318

AFSHIN NAMIRANIAN[1], MOHAMMAD NOAPARAST[1*],
SIED ZIAEDIN SHAFAEI TONKABONI[1]

SEPARATION OF MOLYBDENITE FROM CHALCOPYRITE, USING GRAPHENE OXIDE AS A NOVEL DEPRESSANT

In this research, graphene oxide was introduced as an efficient flotation reagent for the selective separation of molybdenite from chalcopyrite. The performance of graphene oxide and its adsorption mechanism on chalcopyrite were investigated by flotation tests, FTIR spectra, and XPS measurements. First, graphene oxide was synthesised, and then its performance was evaluated by SEM, XRD, and EDX. Flotation tests were carried out in a hallimond flotation cell with a volume of 300 ml. Optimum flotation values were achieved at pH = 9 by adding 250 g/t of PAX (Potassium Amyl Xanthate) as a collector and 50 g/t of A65 (Poly Propylene Glycol) as a frother. The results showed high recovery, around 80% for molybdenite, while chalcopyrite was depressed in high amounts by employing 11 kg/t of graphene oxide as a depressant. Compared to common chalcopyrite depressants such as NaHS, Na_2S, and $C_2H_3NaO_2S$, graphene oxide had a higher potency in depressing, which can be applied as a green-depressant in the separation of molybdenite from chalcopyrite by the flotation process. Also, the validity of the depressing effect on chalcopyrite was verified by XPS and FTIR spectra.

Keywords: Graphene oxide; Chalcopyrite; Flotation; Separation; Molybdenum

1. Introduction

Knowing that Molybdenite is naturally more floatable than Chalcopyrite, Chalcopyrite can be inhibited by a copper depressant such as sodium sulphide, sodium hydrosulphide, cyanide, and Nokes reagents. These depressants selectively prevent the absorption of the collector on chalcopyrite or enhance the chalcopyrite hydrophilicity during the separation process [1-2]. Some general and unexpected problems are associated with using these depressant compounds on mine

[1] UNIVERSITY OF TEHRAN, AMIRABAD-SHOMALI, KOOYE DANESHGAH, 1915656535, TEHRAN, IRAN

* Corresponding author: noparast@ut.ac.ir

sites, such as pipeline corrosion, toxicity, and a high dosage requirement, which result in high capital costs and poor selectivity [3]. As a result, considering the environmental and industrial protection scenarios, it is necessary to consider developing brand-new, non-toxic, and selective compounds to replace these reagents with poor selectivity, high toxicity, and high dosages.

In order to overcome these disadvantages, many modern depressants such as pseudo glycolic thiourea acid [4], acetic acid-[(hydrazinyl thioxomethyl) thio]-sodium [5], 2, 3-disulfanylbutanedioic acid [6], 4-amino-5-mercapto-1, 2, 4-triazole [7], Fenton-like oxidation reagent [8], chitosan [9], thiocarbono hydrazide [10], 4-amino-3-thioxo-3, 4-dihydro-1, 2, 4-triazin-5 (2H)-one [11], disodium bis (carboxymethyl) trithiocarbonate [12], acrylamide-allyl thiourea [13], and carboxymethylcellulose [14] were introduced. Although these depressants have better selectivity and lower toxicity, they have not been widely used on an industrial scale, and their tests were merely carried out in lab-scale studies. Therefore, developing new organic compounds with lower costs, better selectivity, good stability, and biocompatibility with the environment for separating cu from mo utilising flotation is still a challenging operation that will attract more attention [15-16].

This work studied the graphene oxide used as a green and environmentally friendly depressant for separating Cu-Mo by flotation for developing new reagents with good selectivity.

2. Methodology

2.1. Materials and reagents

This research was conducted using pure Molybdenite and Chalcopyrite supplied by the Sarcheshmeh Copper Plant in Kerman province, Iran. The minerals were purified with the reflotation process in a fraction of –75+35 micrometres. To achieve the desired fraction for further analysis (XRD, XRF), the first d_{80} of Molybdenite and Chalcopyrite was classified with a laser particle sizer, as shown in Fig. 1. The d_{80} class of Molybdenite and Chalcopyrite were 41 and 48.3 micrometres, respectively. Then the classified particles were milled to –10 micrometres using a jet mill for 30 mins. Fig. 2A shows the XRD analysis by the D8-Advance model made by Bruker axs with copper anode radiation with wavelength 1.54 K Kα at 40 kV and 30 mA, which Fig. 2B shows the XRD analysis of Molybdenite. Fig. 2C is the characteristic peak of graphene oxide at an angle of 2θ = 10°, and the chemical composition analysis in Table 1 determined that the molybdenite samples' purity was higher than 90%.

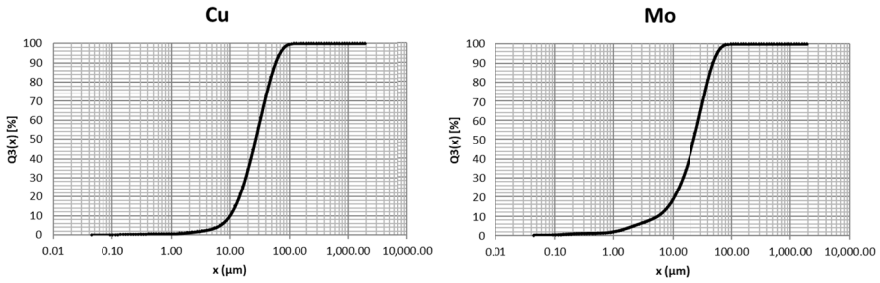

Fig. 1. Particle size distribution graph of pure Chalcopyrite (Cu) and Molybdenite (Mo)

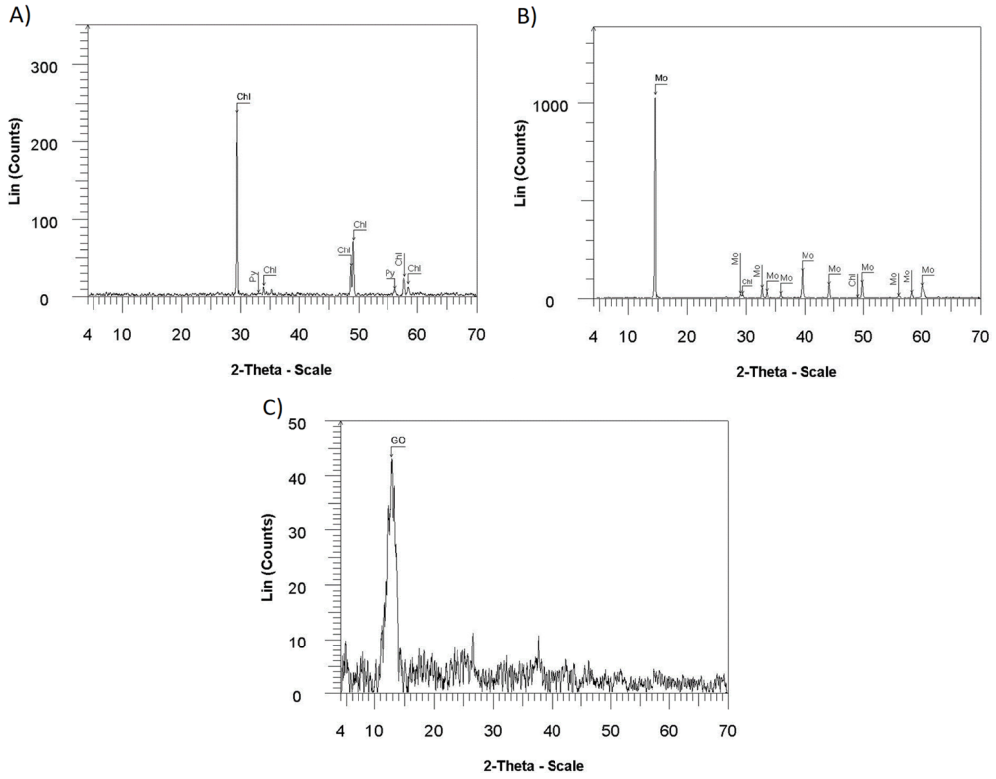

Fig. 2. XRD pattern: A) Chalcopyrite (Chl: Chalcopyrite and py: pyrite); B) Molybdenite (Mo); and C) Graphene oxide (GO)

TABLE 1

Chemical composition analysis of pure Chalcopyrite and Molybdenite

Chemical components	Cu %	Mo %	S %	Fe %	SiO_2 %	CaO %	MgO %	Al_2O_3 %	TiO_2 %
Chalcopyrite	31.45	—	34.36	29.59	1.75	0.14	0.52	0.85	0.122
Molybdenite	1.09	54.29	38.61	2.01	1.78	0.26	0.20	0.45	0.011

2.2. Graphene Oxide

To create graphene oxide for studies utilising the Modified Hummers Method, 2 g of graphite (graphite powder) was first added to 10 ml of concentrated sulphuric acid (98%) while being magnetically agitated. The solution was then mixed with 2 g of potassium persulfate ($K_2S_2O_8$) and 2 g of diphosphate pentoxide (P_2O_5) to preoxidised graphite. A magnetic stirrer agitated the solution for 8 hours at 80°C (in an oil bath). The solution was kept stationary with dilute distilled water for 30 minutes to settle the graphite powder without agitation. To produce graphene oxide, 2 g of the preoxidised graphite was added to 100 ml of concentrated sulphuric acid (98%), and at a low temperature, it was stirred with a magnetic stirrer (300 rpm). Then, 6 g of potassium

permanganate ($KMnO_4$) was slowly added to the mixture, and the reaction temperature was set to 35°C for 6 hours. The reaction mixture was transferred to a 1000 ml container for washing, and 200 ml of distilled water was added to the reaction medium. Afterwards, the precipitated sample was loaded into falcons and placed in a centrifuge with a speed of 4000 rpm for 10 minutes which was washed with 1 M hydrochloric acid. Graphene oxide was dispersed in 400 ml distilled water and exposed to ultrasound waves for 2 hours in three stages.

2.3. Flotation test

The modified hallimond tube with the capacity of 300 ml was employed to perform the flotation tests, as shown in Fig. 3A. Molybdenite and chalcopyrite flotation was tested without the use of a collector and in the absence of depressant and frother at neutral pH for 1, 3, 5, 7, and 9 minutes and the optimal time was determined (5 min). Even knowing that Molybdenite is naturally hydrophobic, PAX (Potassium Amyl Xanthate) and SIPX (Sodium Isopropyl Xanthate) was used as a collector in concentrations of 50, 150, 250, 350, and 450 g/t achieving better flotation results. The PAX collector was chosen as the optimal collector at a concentration of 250 g/t. Meanwhile, 5 g of Molybdenite was utilised in the modified hallimond tube with an optimal amount of PAX and SIPX at pH 2, 4, 6, 9, 10, and 12. Then, to optimise the frother, two frothers A65 (Poly Propylene Glycol) and MIBC (Methyl Isobutyl Carbinol), in concentrations of 25, 50, 75, 100, and 125 g/t in neutral pH and the absence of depressant and A65 with a concentration of 50 g/t was selected as the optimal frother. After determining the optimised values of effective parameters in the molybdenite flotation process, the chalcopyrite concentrate was chosen for the experiments, shown in Fig 3B. With the goal of depressing Chalcopyrite, the optimum amount of graphene oxide in the hallimond tube was determined according to the weight recovery.

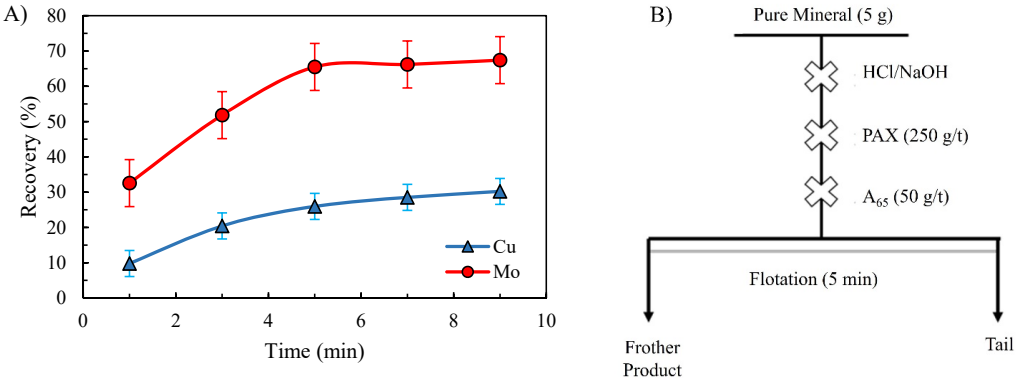

Fig. 3. A) Recovery of Molybdenite and Chalcopyrite (No collector, no frother, no depressor in ambient pH), B) Designed flowsheet of the flotation process

2.4. SEM and EDX Analysis of Graphene oxide

Analysing the surface morphology of graphene oxide was done by VEGA TS 5136 MM device, which the TESCAN company manufactured. For this purpose, five samples were fully

covered in Au-Pd coating rounds. As shown in Fig. 4, the results indicate that the formation of graphene oxide was uniform. A hexagonal and crystalline shape showed that the oxygen groups were present on its surface. Fig. 5 shows graphite and graphene oxide's rectangular point analysis (EDX). Also, the element analysis of graphene oxide is presented in Table 2.

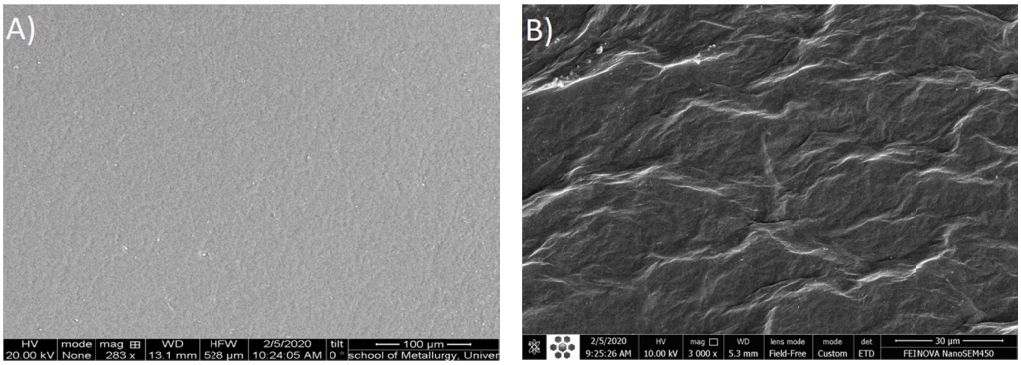

Fig. 4. A) The electron microscope image of graphene oxide with a magnification of 283× and 1/13 mm as the depth of field value. The image indicates the formation of the graphene oxide in a uniform plane; B) The electron microscope image of graphene oxide with the magnification of 3000× and 3/5 mm as the depth of field value. The image indicates the formation of a graphene oxide similar to the texture of cloth

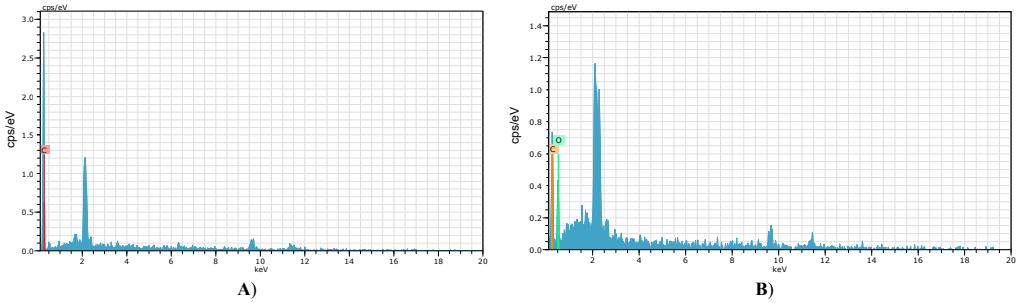

Fig. 5. Results of the rectangular point analysis (EDX) are shown for A) only carbon element can be seen in the peak, which represents pure graphite; and B) two elements of oxygen and carbon can be seen, which represents the transformation of graphite into graphite oxide (C: Carbon, O: Oxygen)

TABLE 2

Results of graphene oxide element analysis

Elements		Grade (%)
Graphite	Carbon	100
Graphene oxide	Oxygen	50.04
	Carbon	49.96

2.5. FT-IR measurements

FT-IR can describe adsorbed species' interactions onto the adsorbent surface; however, adsorption properties do not belong to adsorbed species but to the adsorbent itself. To study changes in mineral surfaces (Molybdenite and Chalcopyrite) before and after processing with graphene oxide, FT-IR analysis for 13 samples. This included Molybdenite and Chalcopyrite processed with graphene oxide in pH 2, 9, 12, graphene, pure graphene oxide, Molybdenite, and Chalcopyrite was carried out by AVATAR machine manufactured in Thermo Company. The mentioned machine was equipped with a high-resolution detector (DigiTech TM), and the operated imaging was done in the wavelength range of 400-4000 cm^{-1}. Approximately 6 mg of each sample was mixed with 200 mg of potassium bromide. After that, a pressing machine prepared tablets of 13 mm in diameter and thickness of 1-2 mm for the FT-IR analysis. It is worth mentioning that potassium bromide lacks a peak in the range of measurements after the pressing process.

2.6. XPS measurements

XPS analysis is widely used in mineral engineering to describe the composition of elements and the state of minerals and uncover the interaction mechanism of reagents and minerals. In this study, XPS analysis was performed by a German Bes Tec machine in 10-10 mbar vacuum condition with the aluminium anode (1486ev) in Sharif Industrial University's lab. XPS analysis for all the samples processed by flotation was accomplished at a pH of 9.

3. Results and Discussion

3.1. Flotation Optimization Tests

Molybdenite and chalcopyrite recoveries were investigated without depressants by applying different collectors at different concentrations (Fig. 6). The recovery of Molybdenite was tested with PAX (Potassium Amyl Xanthate) and SIPX (Sodium Isopropyl Xanthate) in a pH

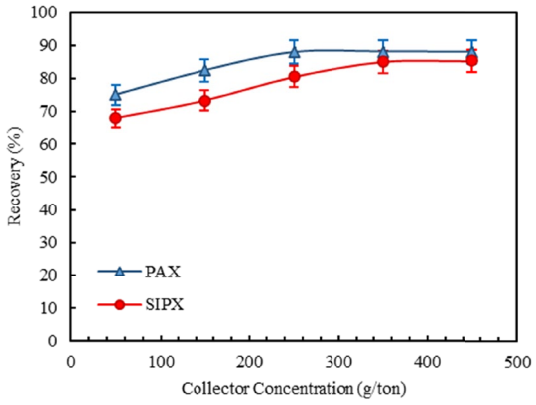

Fig. 6. Recovery of Molybdenite using PAX and SIPX in the absence of depressant

environment, as the abilities of the collectors could be measured. Due to the length and size of the hydrocarbon chain, PAX generally indicates a higher ability to make the mineral particles floatable. Different concentrations of collectors were also selected to evaluate their impact on the flotation process. It is also noted that increasing the concentration of the collector would usually be constant when achieving maximum recovery.

Investigated were the recoveries of molybdenite and chalcopyrite in optimum collector conditions utilising various frother types and concentrations without depressant of the pH environment (Fig. 7). Molybdenite and chalcopyrite flotation test were performed to choose the type and optimal amount of frother with these conditions: frothing time equal to 5 minutes, collector (PAX = 250 g/t) in neutral pH and without depressor. A65 (Poly Propylene Glycol) can produce finer and more stable bubbles, leading to a higher flotation recovery.

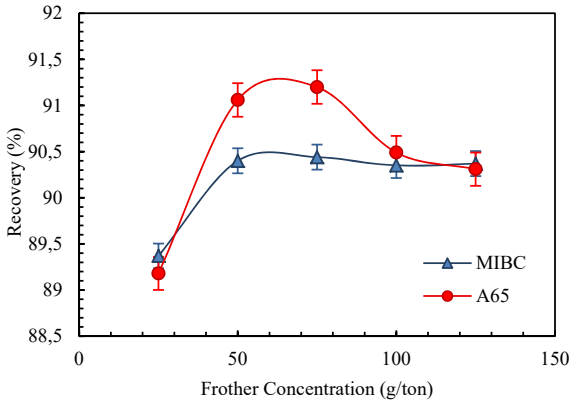

Fig. 7. Recovery comparison of Molybdenite using A65 and MIBC (Methyl Iso Butyl Carbinol) as frothers in the absence of depressant

The recoveries of Molybdenite and Chalcopyrite with the assistance of PAX and A65 were investigated in the presence and absence of a depressant (Graphene Oxide) as a function of pH (Fig. 8). In the absence of a depressant, molybdenum recovery has increased in acidic pH and decreased in basic pH, which OH^- ions in solution may cause the effect. In addition, the same conditions happened to the recovery of Chalcopyrite. Due to the optimal conditions in the presence of a depressant, the recovery values were measured in various pH values. As shown in Fig. 8B, it is clear that at a pH of 9, maximum recovery for Molybdenite can be achieved while Chalcopyrite is depressed at its highest amount. It can be concluded that Molybdenite presented higher recoveries in the absence of depressants for a wide range of pH 2-10. The recovery of copper also followed the same trend. However, after the addition of depressant, while the copper recovery decreased almost twofold, the recovery of Molybdenite started from 40 to around 90 at higher pH values. Yet, it declined to a minimum of 70%, which is higher than other conditions.

3.2. Depressant effect

The effects of graphene oxide on molybdenite flotation were investigated by designing experiments to optimise the effective factors such as frothing time, collector, frother types,

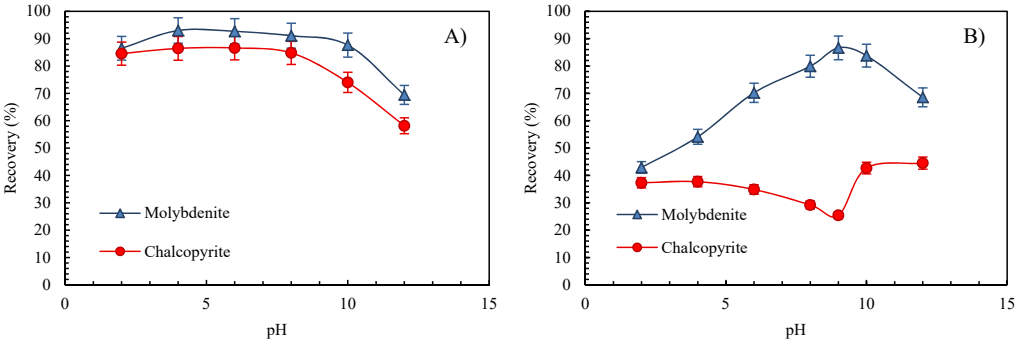

Fig. 8. Comparison of molybdenite and chalcopyrite recoveries in A) Flotation time is 5 min, collector (PAX = 250 g/t), frother (A65 = 50 g/t), flotation test was done in different pH and without a depressant to get optimal pH and B) The flotation time is 5 min, the collector (PAX = 250 g/t), frother (A65 = 50 g/t), and in the presence of graphene oxide depressant with the optimal amount of 11000 g/ton, the flotation test was performed at different pH. The results show that at pH = 9, maximum recovery for Molybdenite can be achieved while Chalcopyrite is depressed at its highest amount

concentrations, and pH. In these experiments, 5 minutes of frothing time, about 250 g/t of PAX as a collector, 50g/t of A65 as a frother, and pH = 9 were obtained as optimised values for each factor, respectively.

According to the optimum conditions, a flotation test with the optimal collector (PAX = 250 g/t), optimal frother (A65 = 50 g/t), frother time equal to 5 minutes, and pH = 9 was conducted. These values were applied at different concentrations of a depressant to represent the direct effects of graphene oxide on the weight recovery of Chalcopyrite and Molybdenite (Fig. 9). The results indicated that by increasing the graphene oxide concentration, the depression mechanism works well on Chalcopyrite as weight recovery decreases. The optimal amount of depressor (graphene oxide) was 11000 g/t.

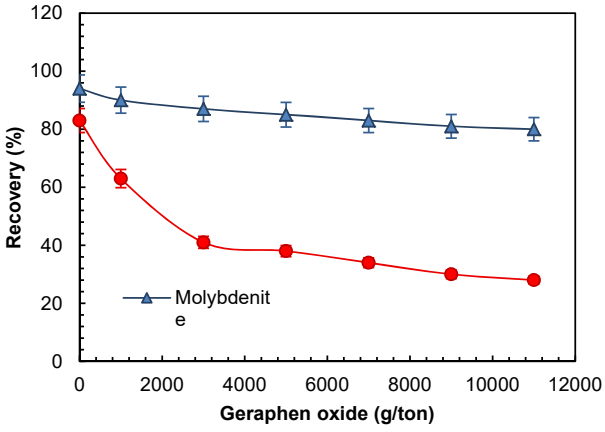

Fig. 9. The depressing effect of graphene oxide at various concentrations on Molybdenite and Chalcopyrite

3.3. FTIR Analysis

To specify the adsorption mechanism of graphene oxide on the surface of Chalcopyrite, the FT-IR spectrum of graphene oxide and the pure and processed Chalcopyrite were compared (Fig. 10). As shown in Fig. 10A, the peak of 1729 cm^{-1} appeared in graphene oxide's spectrum, which was assigned to the stretching vibrations of the C=O (aldehyde group) in the graphene oxide's structure. The peak at about 1671 cm^{-1} belonged to the tensile vibrations of C=C in the main chain of the graphene oxide. Moreover, three peaks at about 500 cm^{-1}, 700 cm^{-1}, and 1027 cm^{-1} were observed, which were related to the stretching vibrations of S=O, C-S, and S-S groups, respectively (Table 3). In Fig. 10C, there is a sharp peak for the processed Chalcopyrite with graphene oxide, whereas, in the pure sample, this peak is missing since adsorption accrued. It can be inferred that there is an interaction between the metallic group and graphene oxide, which proved the adsorption of graphene oxide on Chalcopyrite's surface. By comparing Fig. 10B and

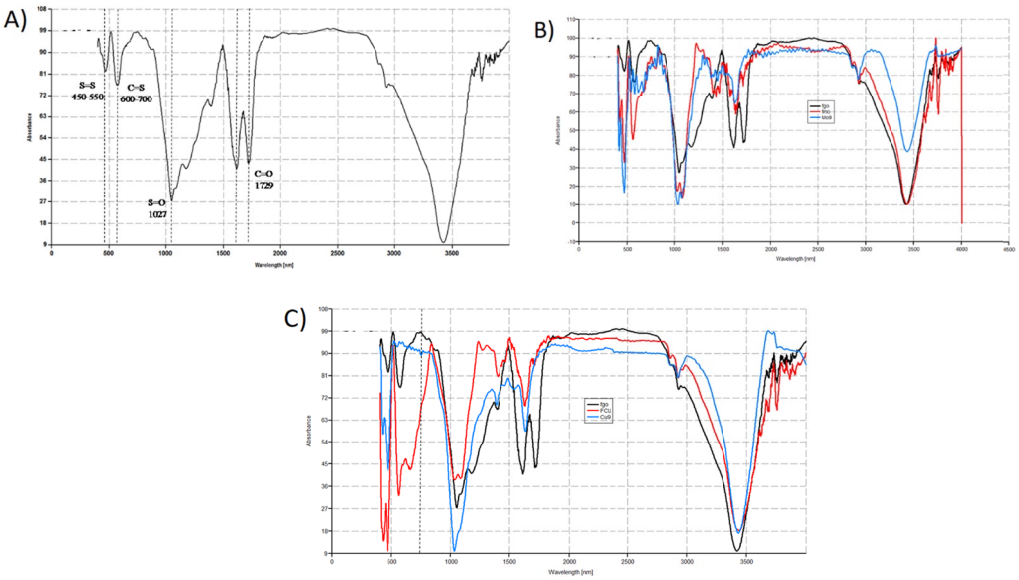

Fig. 10. FT-IR analysis of the sample, A) graphene oxide, B) processed Molybdenite (Pure Molybdenite (red), graphene oxide (black), and processed Molybdenite with graphene oxide at pH 9 (blue)), C) processed Chalcopyrite (Pure Chalcopyrite (red), graphene oxide (black) and processed Chalcopyrite with graphene oxide at pH 9 (blue))

TABLE 3

The wavenumbers observed in FTIR diagrams and the type of bonds associated with them (M * stands for metal) [17]

Bond type	Wavenumber (cm^{-1})	Bond type	Wavenumber (cm^{-1})
C-S tensional	600-700	S = O tensional	(1060-1020) 1027
S-S tensional	450-550	C = C tensional	1671
M^* = O tensional	850-1010	C = O tensional	1729

Fig. 10C, it appears that in pH = 9, graphene oxide has absorbed significantly on Chalcopyrite's surface, and it causes Molybdenite to be well-floated.

3.4. XPS Analysis

Analysing the chemical composition of the sample's surface and its structure was performed by X-ray Spectroscopy Analysis (XPS), which is a detailed and advanced analysing method for measuring and determining the chemical composition of the samples, including their type of bonding [18]. All the related XPS analyses for the test samples were carried out at pH = 9.

As shown in Fig. 11, a pure chalcopyrite sample was analysed in detail ($CuFeS_2$) which in the XPS spectra related to Cu 2p (Fig. 11B), two separated peaks were observed in Cu 2p3/2

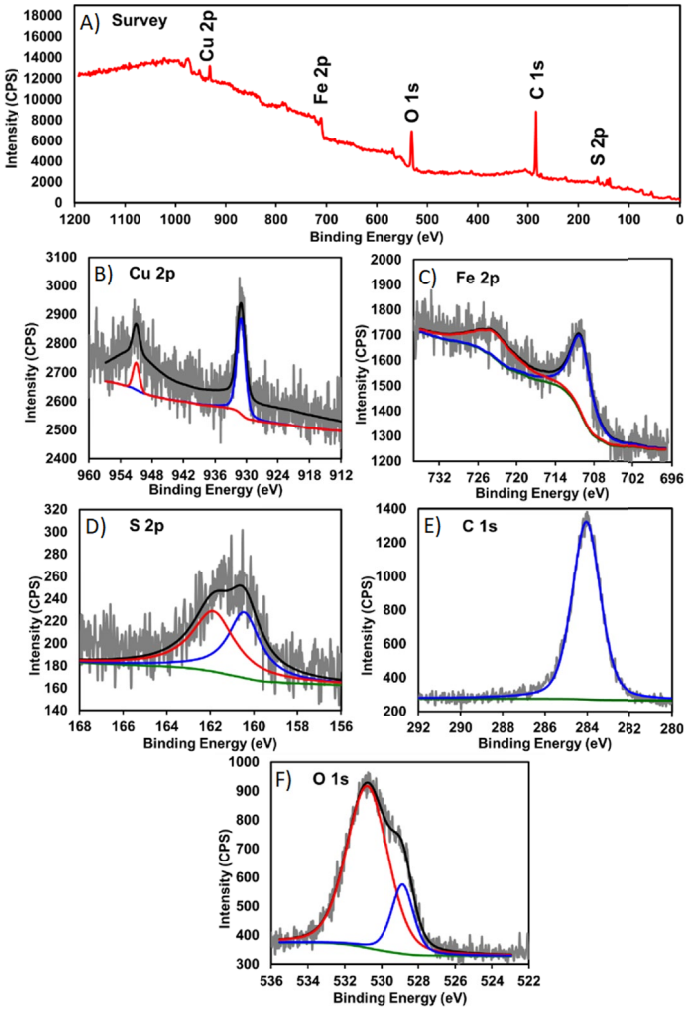

Fig. 11. A) XPS comprehensive curve, B) Cu 2p spectrum, C) Fe 2p spectrum, D) S 2p spectrum

and Cu 2p1/2 with the bonding energy of 931.1 and 951eV, respectively [19]. The exact value of orbit-spin fission for this metal was 19.90eV, the same as the amount reported in the literature [20]. In the XPS spectra of Fe-2p (Fig. 11C), two separated peaks of Fe 2p3/2 and Fe 2p1/2 were recognized with the bonding energies of 710 and 723eV, respectively. The exact value of orbit-spin fission was reported to be 13eV [21]. In the XPS spectra associated with the sulphur element (S 2p) for this test sample (Fig. 11D), two separated peaks related to S 2p3/2 and S 2p1/2 were also witnessed with bonding energies 160.40 and 161.80eV with an orbit-spin fission value of 1.40eV.

According to Fig. 12, pure Molybdenite (MoS2) spectra were discussed in detail, wherein XPS spectra of Mo 3d (Fig. 12B), the two separated peaks related to Mo 3d5/2 and Mo 3d3/2 were observed with bonding energies of 228.60 and 231.80eV, respectively. Additionally, the exact value of orbit-spin fission for this metal was calculated to be 3.20eV, which is similar to the reported value by Zhang et al. [22]. XPS spectra associated with the sulphur element (S 2p) for this test sample (Fig. 12C) also showed two separated peaks corresponding to S 2p3/2 and S 2p1/2 with the bonding energies of 161.40 and 162.60eV, respectively. The value of orbit-spin fission for this structure was 1.20eV, similar to literature reports [23].

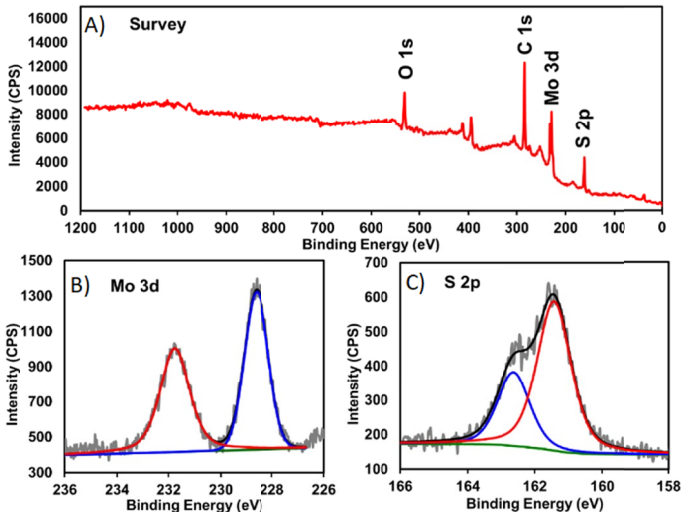

Fig. 12. A) XPS comprehensive curve, B) Mo3d spectrum, C) S 2p Spectrum for pure molybdenite

Fig. 13 shows the XPS analysis of graphene oxide, in which, in its comprehensive curve (Fig. 13A), two indices' peaks related to carbon and oxygen atoms are specified. In the XPS spectra of C 1s (Fig. 13B), after the peak splitting and its fitting process, it is entirely understandable that this peak consists of three distinct components or peaks observed in bonding energies of 281.60, 283.75, and 285.50eV. These three peaks are C=C, C-O, and C=O [24]. XPS spectrum of the oxygen element (O 1s) for this test sample (Fig. 13C) consists of three separated peaks C=C-O, C-C, and C=O. Their bonding energies are 528.75, 529.80, and 530.40eV, respectively, documented in the literature [25].

After processing molybdenite and chalcopyrite samples with graphene oxide at pH = 9 utilising the flotation method, processed samples were then investigated by XPS analysis. XPS analysis

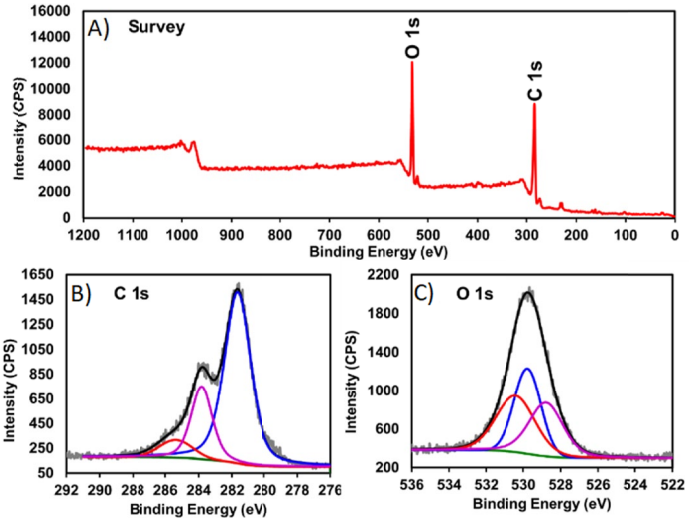

Fig. 13. A) XPS comprehensive curve, B) C 1s spectrum, and C) O 1s spectrum for Graphene oxide sample

results for the processed chalcopyrite samples are shown in Fig. 14. XPS spectra of Cu 2p3/2 and Cu 2p1/2 were obtained at the bonding energy amounts of 931.20 and 951.30eV, respectively. The exact value of orbit-spin fission for this metal was 20.10eV. This increase describes the changes in electronic density around copper, indicating copper's attachment to graphene oxide. Fe 2p's XPS spectrum for this test was similarly two separated peaks related to Fe-2p3/2 and Fe-2p1/2 with the bonding energies of 710.80 and 724.50eV, respectively. Further increase in the amount of orbit-spin fission for iron compared to copper indicates the higher affinity of graphene oxide's functional groups for attaching to iron. XPS spectrum related to the sulphur element (S-2p). In this test (Fig. 14D), two separated peaks for S 2p3/2 and S 2p1/2 were also formed with the bonding energies of 160.30 and 161.40eV, respectively, while the orbit-spin fission was 1.10eV. The reduction of orbit-spin fission value for the sulphur element in the processed sample to pure Chalcopyrite indicates that in chalcopyrite structure, several metal-sulphur bonds are replaced with metal-oxygen bonds caused by bonding oxygenated functional groups of graphene to Chalcopyrite's surface. In carbon and oxygen spectra (Fig. 14E and Fig. 14F), the presence of graphene oxide components indicates the bonding between chalcopyrite and graphene oxide [2].

The results of the XPS analysis for the molybdenite sample after flotation using graphene oxide are shown in Fig. 15. In XPS spectra of Mo 3 d (Fig. 15B), two separated peaks related to Mo 3d5/2 and Mo 3d3/2 were observed with bonding energies of 228.50 and 231.70eV, respectively. The value of orbit-spin fission was 3.20eV. The XPS spectra of the sulphur element (S 2p) for this sample (Fig. 15C) consisted of two separated peaks corresponding to S 2p3/2 and S 2p1/2 with the bonding energies 161.40 and 162.50eV, respectively, and the orbit-spin value was 1.10eV. There were no noticeable changes in molybdenum and sulphur orbit-spin values, indicating that the structure is unwilling to bond with graphene oxide's functional groups [26].

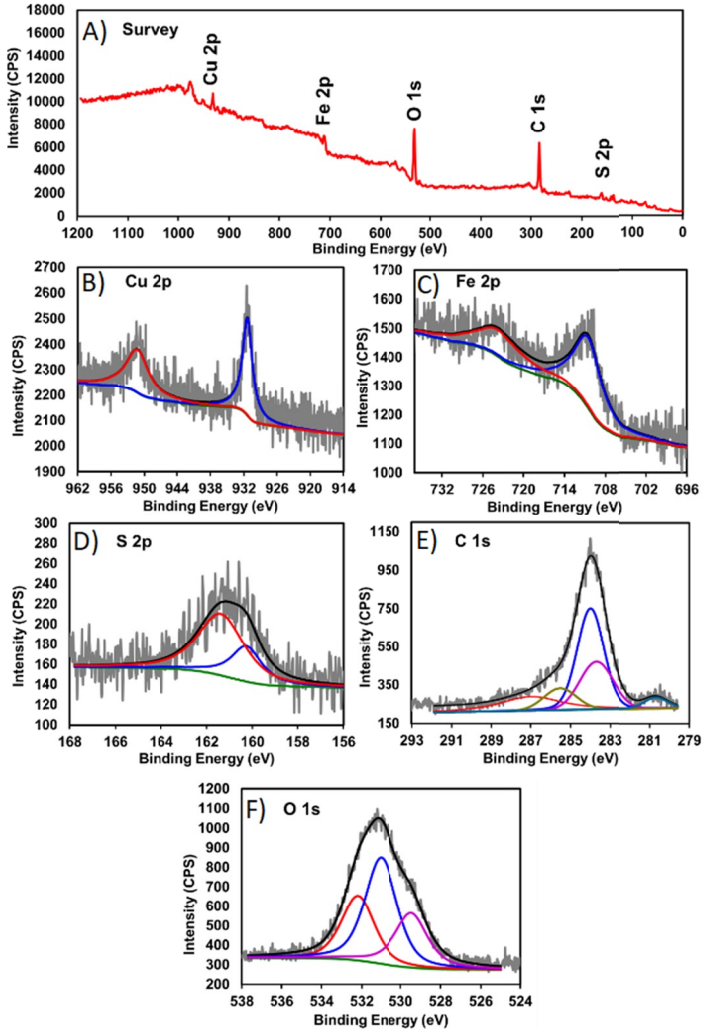

Fig. 14. A) XPS comprehensive curve, B) Cu 2p spectrum, C) Fe 2p spectrum, D) S 2p spectrum, E) C 1s spectrum, and F) O 1s spectrum for processed chalcopyrite with graphene oxide at pH = 9

4. Conclusions

In the present study, graphene oxide was synthesised and verified by SEM, XRD, and EDX. The composition of molybdenite concentrate was subjected to the separation of Molybdenite from Chalcopyrite. FTIR and XPS analysis evaluated the absorption mechanisms of graphene oxide to Molybdenite and Chalcopyrite. Based on the observations, the following results were obtained:

Graphene oxide has a high impact on depressing Chalcopyrite. Therefore, the separation of Molybdenite from Chalcopyrite can be achieved under the weak alkaline condition at a pH equal to 9 by adding 250 g/t PAX as a collector and 50 g/t of A65 as a frother.

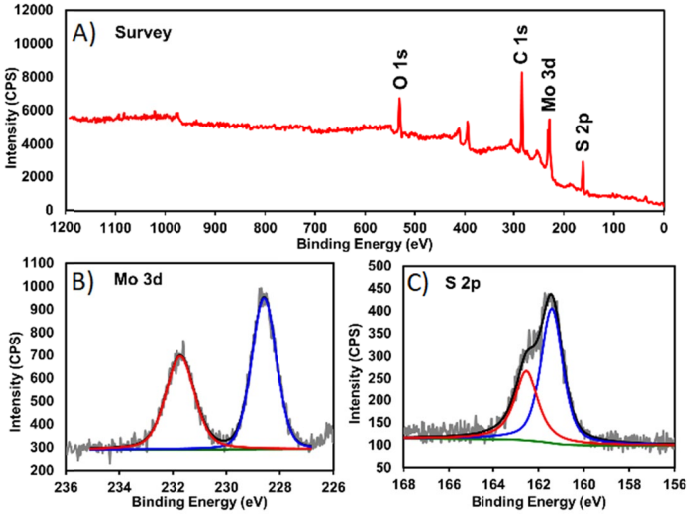

Fig. 15. A) XPS comprehensive curve, B) Mo 3d spectrum and C) S 2p Spectrum for processed Molybdenite with graphene oxide at pH = 9

The flotation results indicated that Mo/Cu selectivity index was significantly improved when graphene oxide was used as a potential chalcopyrite depressant in laboratory-scale experiments. Also, the results showed that molybdenum recovery could reach up to 80% when 11000 g/t of graphene oxide was employed as a depressant.

FTIR and XPS results proved that graphene oxide could form copper complexes with copper ions in about 850 cm^{-1}. However, the possible physical adsorption mechanism of graphene oxide on the surface of Molybdenite may be controlled by hydrogen bonds or van der Waals forces. XPS spectra of Cu 2p3/2 and cu2p1/2 were obtained at the bonding energy amounts of 931.20 and 951.30eV, respectively. The exact value of orbit-spin fission for this metal was 20.10eV. This increase describes the changes in electronic density around copper, which indicates the attachment of copper to graphene oxide.

Abbreviations

Potassium Amyl Xanthate	PAX
Poly Propylene Glycol	A65
Sodium Isopropyl Xanthate	SIPX
Graphene oxide	GO
Gold	Au
X-ray Spectroscopy Analysis	XPS
Chalcopyrite	Chl
pyrite	py
Molybdenite	mo
Copper	cu
Palladium	Pd

References

[1] S. Castro, A. Lopez-Valdivieso, J. Laskowski, Review of the flotation of Molybdenite. Part I: Surface properties and floatability. Int. J. Miner. Process. **148**, 48-58 (2016). DOI: https://doi.org/10.1016/j.minpro.2016.01.003

[2] B. Yang, H. Yan, M. Zeng, P. Huang, F. Jia, A. Teng, A novel copper depressant for selective flotation of Chalcopyrite and Molybdenite. Miner. Eng. **151**, 106309 (2020). DOI: https://doi.org/10.1016/j.mineng.2020.106309

[3] J.A. Peterson, M.S. Saran, J.S. Wisnouskas, Differential flotation reagent for molybdenum separation. ed: Google Patents, (1986).

[4] J.-H. Chen, L.-H. Lan, X.-J. Liao, Depression effect of pseudo glycolythiourea acid in flotation separation of copper-molybdenum. T. Nonferr. Metal. Soc. **23** (3), 824-831 (2013). DOI: https://doi.org/10.1016/S1003-6326(13)62535-2

[5] Z. Yin, W. Sun, Y. Hu, C. Zhang, Q. Guan, R. Liu, P. Chen, M. Tian, Utilization of acetic acid-[(hydrazinylthioxomethyl) thio]-sodium as a novel selective depressant for Chalcopyrite in the flotation separation of Molybdenite. Sep. Purif. Technol. **179**, 248-256 (2017). DOI: https://doi.org/10.1016/j.seppur.2017.01.049

[6] M.-Y. Li, D.-Z. Wei, Y.-B. Shen, W.-G. Liu, S.-L. Gao, G.-G. Liang, Selective depression effect in flotation separation of copper-molybdenum sulfides using 2, 3-disulfanylbutanedioic acid. T. Nonferr. Metal. Soc. **25** (9), 3126-3132 (2015). DOI: https://doi.org/10.1016/S1003-6326(15)63942-5

[7] Z. Yin, Y. Hu, W. Sun, C. Zhang, J. He, Z. Xu, J. Zou, C. Guan, C. Zhang, Q. Guan, Adsorption mechanism of 4-amino-5-mercapto-1, 2, 4-triazole as flotation reagent on Chalcopyrite. Langmuir. **34** (13), 4071-4083 (2018). DOI: https://doi.org/10.1021/acs.langmuir.7b03975

[8] G.P.W. Suyantara, T. Hirajima, H. Miki, K. Sasaki, M. Yamane, E. Takida, S. Kuroiwa, Y. Imaizumi, Effect of Fenton-like oxidation reagent on hydrophobicity and floatability of Chalcopyrite and Molybdenite. Colloid. Surface. A. **554**, 34-48 (2018). DOI: https://doi.org/10.1016/j.colsurfa.2018.06.029

[9] M. Li, D. Wei, Q. Liu, W. Liu, J. Zheng, H. Sun, Flotation separation of copper–molybdenum sulfides using chitosan as a selective depressant. Miner. Eng. **83**, 217-222 (2015). DOI: https://doi.org/10.1016/j.mineng.2015.09.013

[10] C. Guan, Z. Yin, S. Ahmed Khoso, W. Sun, Y. Hu, Performance analysis of thiocarbonohydrazide as a novel selective depressant for Chalcopyrite in molybdenite-chalcopyrite separation. Mineral-Basel. **8** (4), 142 (2018). DOI: https://doi.org/10.3390/min8040142

[11] Z. Yin, W. Sun, Y. Hu, C. Zhang, Q. Guan, C. Zhang, Separation of Molybdenite from Chalcopyrite in the Presence of Novel Depressant 4-Amino-3-thioxo-3, 4-dihydro-1, 2, 4-triazin-5 (2H)-one. Mineral-Basel. **7** (8), 146 (2018). DOI: https://doi.org/10.3390/min7080146

[12] Z.-G. Yin, S. Wei, Y.-H. Hu, Q.-J. Guan, C.-H. Zhang, Y.-S. Gao, J.-H. Zhai, Depressing behaviors and mechanism of disodium bis (carboxymethyl) trithiocarbonate on separation of Chalcopyrite and Molybdenite. T. Nonferr. Metal. Soc. **27** (4), 883-890 (2017). DOI: https://doi.org/10.1016/S1003-6326(17)60100-6

[13] X. Zhang, L. Lu, Y. Cao, J. Yang, W. Che, J. Liu, The flotation separation of Molybdenite from Chalcopyrite using a polymer depressant and insights to its adsorption mechanism. Chem. Eng. J. **395**, 125137 (2020). DOI: https://doi.org/10.1016/j.cej.2020.125137

[14] X. Qiu, H. Yang, G. Chen, W. Luo, An alternative depressant of Chalcopyrite in Cu-Mo differential flotation and its interaction mechanism. Mineral-Basel. **9** (1), 1 (2018). DOI: https://doi.org/10.3390/min9010001

[15] P. Duda, R. Muzyka, Z. Robak, S. Kaptacz, Mechanical properties of graphene oxide-copper composites. Arch. Metall. Mater. **2**, 863-868 (2016). DOI: http://dx.doi.org/10.1515/amm-2016-0146

[16] A. Baran, M. Śliwka, M. Lis, Selected Properties of Flotation Tailings Wastes Deposited in the Gilów and Żelazny Most Waste Reservoirs Regarding Their Potential Environmental Management/Wybrane Właściwości Odpadów Poflotacyjnych Zdeponowanych w Zbiornikach Gilów i Żelazny Most w Aspekcie Możliwości Ich Zagospodarowania Przyrodniczego. AMS, **3** (2013). DOI: http://dx.doi.org/10.2478/amsc-2013-0068

[17] G. Jozanikohan, M.N. Abarghooei, The Fourier transform infrared spectroscopy (FTIR) analysis for the clay mineralogy studies in a clastic reservoir. J. Pet. Explor. Prod. Technol. 1-14, (2022). DOI: https://doi.org/10.1007/s13202-021-01449-y

[18] O. Sublemontier, C. Nicolas, D. Aureau, M. Patanen, H. Kintz, X. Liu, M.-A. Gaveau, J.-L. Le Garrec, E. Robert, F.-A. Barreda, X-ray photoelectron spectroscopy of isolated nanoparticles. J. Phys. Chem. Lett. **5** (19), 3399-3403 (2014). DOI: https://doi.org/10.1021/jz501532c

[19] X. Xu, D. Tang, J. Cai, B. Xi, Y. Zhang, L. Pi, X. Mao, Heterogeneous activation of peroxymonocarbonate by Chalcopyrite (CuFeS2) for efficient degradation of 2, 4-dichlorophenol in simulated groundwater. Appl. Catal. B-Environ. **251**, 273-282 (2019). DOI: https://doi.org/10.1016/j.apcatb.2019.03.080

[20] A. Ghahremaninezhad, D. Dixon, E. Asselin, Electrochemical and XPS analysis of Chalcopyrite (CuFeS2) dissolution in sulfuric acid solution. Electrochim. Acta. **87**, 97-112 (2013). DOI: https://doi.org/10.1016/j.electacta.2012.07.119

[21] P. Velásquez, H. Gómez, J. Ramos-Barrado, D. Leinen, Voltammetry and XPS analysis of a chalcopyrite CuFeS2 electrode. Colloid. Surface. A. **140** (1-3), 369-375 (1998). DOI: https://doi.org/10.1016/S0927-7757(97)00293-8

[22] X. Zhang, L. Lu, H. Zeng, Z. Hu, Y. Zhu, L. Han, A macromolecular depressant for galena and its flotation behavior in the separation from Molybdenite. Miner. Eng. **157**, 106576 (2020). DOI: https://doi.org/10.1016/j.mineng.2020.106576

[23] B. Yang, H. Yan, M. Zeng, H. Zhu, Tiopronin as a novel copper depressant for the selective flotation separation of Chalcopyrite and Molybdenite. Sep. Purif. Technol. **266**, 118576 (2021). DOI: https://doi.org/10.1016/j.seppur.2021.118576

[24] R. Al-Gaashani, A. Najjar, Y. Zakaria, S. Mansour, M. Atieh, XPS and structural studies of high quality graphene oxide and reduced graphene oxide prepared by different chemical oxidation methods. Ceram. Int. **45** (11), 14439-14448 (2019). DOI: https://doi.org/10.1016/j.ceramint.2019.04.165

[25] D. Boukhvalov, I. Zhidkov, A. Kukharenko, S. Cholakh, J.L. Menéndez, L. Fernández-García, E. Kurmaev, Interaction of graphene oxide with barium titanate in composite: XPS and DFT studies. J. Alloy. Compd. **840**, 155747 (2020). DOI: https://doi.org/10.1016/j.jallcom.2020.155747

[26] X. Wang, P. Gao, J. Liu, X. Gu, Y. Han, Adsorption performance and mechanism of eco-friendly and efficient depressant galactomannan in flotation separation of Chalcopyrite and Molybdenite. J. Mol. Liq. **326**, 115257 (2021). DOI: https://doi.org/10.1016/j.molliq.2020.115257